ELSEVIER

Journal of Chromatography A, 693 (1995) 251–261

JOURNAL OF CHROMATOGRAPHY A

Ionic strength dependence of protein retention on Superose 12 in SEC–IEC mixed mode chromatography

Chun-hua Cai, Vincent A. Romano, Paul L. Dubin*

Department of Chemistry, Indiana University–Purdue University, Indianapolis, IN 46202, USA

First received 16 August 1994; revised manuscript received 21 October 1994

Abstract

Protein retention was studied on Superose 12 in SEC–IEC mixed mode, over a wide range of ionic strength (16.8 mM to 500 mM). A new SEC parameter, K_{int}, which is analogous to the capacity factor k' in IEC was defined. The effect of ionic strength on K_{int} was compared to predictions from two previous models, that of Kopaciewicz et al. [1] and that of Ståhlberg et al. [2]. The ionic strength dependence of K_{int} more closely fits the second model, and the stationary phase surface charge density calculated from the model agrees well with the experimental value.

1. Introduction

Ion-exchange chromatography (IEC) is a valuable tool for the analysis and separation of proteins [3]. IEC is a form of liquid chromatography in which retention is governed by Coulomb forces between the solute and the oppositely charged packing. Experimentally, this retention is described by the capacity factor:

$$k' = \frac{t_r - t_0}{t_0} \quad (1)$$

where t_r is the retention time of the given solute and t_0 is that of an unretained solute.

Several mechanisms have been proposed for protein retention in IEC. These models differ greatly at a fundamental level and also predict different dependencies of t_r and thus k' on the ionic strength (I). Boardman and Partridge [4] (later referred to as BP) proposed a simple mass-action model which treated the protein as a multivalent ion that displaces a well-defined number of ions on the packing surface corresponding to the "valency" of the protein. Kopaciewicz et al. [1] (later referred to as KRFR) extended this model to include the effect of small ions. Their treatment leads to a linear dependence of log k' on log $1/I$ with a slope related to the number of ions needed to displace the protein from the stationary phase. More recently, Ståhlberg et al. [2] (SJH) proposed a non-stoichiometric model and consequently suggest the term "electrostatic interaction chromatography" for proteins in place of ion-exchange chromatography. The SJH model is based on the assumption that the interaction between a protein and an ion-exchange column can be treated as an electrostatic interaction between two oppositely charged surfaces separated by a salt solution. The magnitude of this interaction is obtained by solving the Poisson–Boltzmann equation for two oppositely charged parallel slabs in

* Corresponding author.

0021-9673/95/$09.50
SSDI 0021-9673(94)01064-1

contact with a salt solution. Consequently, SJH predicted a linear relation between ln k' and $1/\sqrt{I}$ which was supported experimentally. The net charge of the protein may be calculated using the slope and some fundamental physico-chemical constants.

There are several problems associated with the foregoing models. The KRFR model does not take into account the charge density of the column packing. It also provides an unrealistic stoichiometry in that each protein charge must interact with a complementary packing charge. Finally, the role of the salt is only as a "displacer"; therefore, screening effects are ignored. The SJH model considers such screening effects but neglects protein charge heterogeneity (charge patches) inasmuch as the protein charges are considered to be smeared over the surface of a sphere, half of which interacts with the packing surface.

Charge heterogeneity is an important consideration in protein chromatography. Kopaciewicz et al. [1] showed that proteins could be retained even when the protein bears a net charge of the same sign as the column, or even zero charge (at the isoelectric point). For example, β-lactoglobulin can be retained one pH unit below its pI on an anion-exchange column, or one-half pH unit above its pI on a cation-exchange column. Six other proteins also show significant retention at their pI value on both anion- and cation-exchange columns. Lesins and Ruckenstein [5] also found significant retention of positively charged proteins on positively charged anion-exchange columns. These studies reveal the effect of protein "charge patches" on retention in IEC.

How can two theories which give different ionic strength dependence of the capacity factor both be supported by experiment? Experiments such as those in Refs. [1] and [2] tend to be conducted over a relatively small range of ionic strength because the practical range of ionic strengths used in IEC is considered to be between 50 mM and 500 mM [4]. Fig. 1 shows that ln $1/I$ and $1/\sqrt{I}$ (the two functions of ionic strength used in Refs. [1] and [2]) are virtually collinear in the range covered by those studies. A clear definition of the relationship between

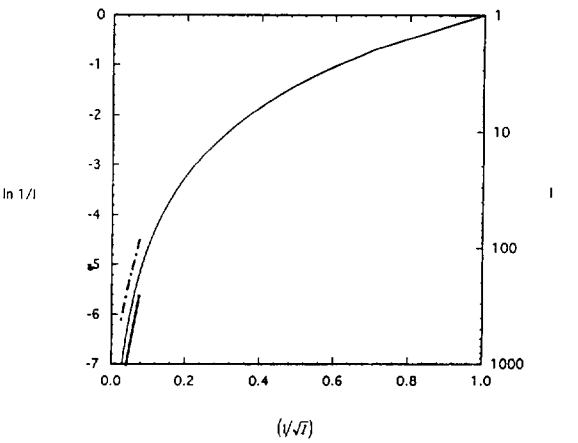

Fig. 1. Hypothetical plot of ln $(1/I)$ versus $(1/\sqrt{I})$ which are the two functions of ionic strength used by the KRFR and SJH models respectively. The ionic strength ranges used to experimentally test the two models are given by the dashed (KRFR) and solid (SJH) lines drawn outside the curve. Ionic strength is given on the right-hand vertical axis for reference.

capacity factor and ionic strength thus requires data over a wider range of ionic strengths. Such studies can be done on weak ion-exchange resins, one example being the packing used in aqueous size exclusion chromatography (SEC).

In ideal SEC, molecules are separated solely on the basis of size, but in non-ideal SEC, electrostatic or hydrophobic interactions contribute to the solute retention. While hydrophobic interactions in protein SEC are relatively weak at low ionic strength, electrostatic effects may contribute significantly to retention. This allows one to use an SEC column as a weak ion exchanger [6].

The chromatographic partition coefficient in SEC is given by:

$$K_{SEC} = \frac{(V_e - V_0)}{(V_t - V_0)} \tag{2}$$

where V_e is the retention volume of the solute, V_0 is the interstitial volume of the column, which is obtained as the retention volume of a solute too large to permeate the pores, and V_t is the total volume of the column, which is obtained as the retention volume of a small solute such as D_2O. For ideal SEC, K_{SEC} is purely dependent on the

dimensions of the solute, R, and the dimensions of the column pores, r_p. From a simple geometric model where the solute is treated as a sphere and the column pore is treated as a slab, cylinder, or sphere, this relationship is given by:

$$K = \left(1 - \frac{R}{r_p}\right)^{\lambda} \quad (3)$$

where $\lambda = 1$, 2, or 3 for slab, cylindrical, or spherical pores respectively [7]. The solute radius, R, generally adopted by protein chemists is the Stokes radius:

$$R_s = \frac{kT}{6\pi\eta D} \quad (4)$$

where R_s is in m, and k is the Boltzmann constant (J/K), T is temperature (K), η is the solvent viscosity (Poise), and D is the diffusion coefficient (m^2/s). A second size parameter more popular among polymer chemists is the viscosity radius [8]:

$$R_\eta = \frac{3[\eta]M}{10\pi N_A}^{1/3} \quad (5)$$

where R_η is in cm, when $[\eta]$ the intrinsic viscosity is in cm^3/g, M the molecular weight is in g/mol, and N_A is Avogadro's number. R_η has been reported to unify the data for globular proteins better than R_S [10]. The relation between K and R is the column calibration curve, which, for cylindrical pores, should appear as a linear plot of $K^{1/2}$ versus R [7]. It should be noted that this last relationship is based on one of many models and is certainly not proven.

In this paper, we study the dependence of protein retention in SEC on the ionic strength over an extended range of ionic strength. We plot our data according to the KRFR and SJH models for the purpose of comparison of the two conflicting models. A method for normalizing size effects in non-ideal SEC is provided in order to isolate the electrostatic contribution. The effect of column packing charge density is also considered.

2. Experimental

2.1. Materials

Table 1 lists protein characteristics, including source, molecular mass, isoelectric point (pI), Stokes radius (R_S), and viscosity radius (R_η), the last being the solute dimension of preference, for reasons noted above. Amine-core, sodium carboxylate polyamidoamine (PAMAM) dendrimers (lot # ZN-SN-A) were gifts from D. Tomalia at the Michigan Molecular Institute and are described in Table 2. Ficoll fractions, obtained from K. Granath of Kabi Pharmacia, are listed in Table 3. Pullulan samples (Shodex Standard P-82 lot # 20101) from Showa Denko K.K. are described in Table 4. All buffers and salts were reagent grade from Sigma, Fisher or Aldrich.

2.2. Methods

Size-exclusion chromatography

A Superose 12 HR 10/30 (Pharmacia) column (12% cross-linked agarose medium) with a typi-

Table 1
Characteristics of proteins used in this study

Protein[a]	Source	M_r	pI	R_S^b (nm)	R_h^c (nm)
RNAse (L-6876)	Bovine pancreas	13 700	9.0	1.8	1.9
Lysozyme (R-5503)	Hen egg white	14 000	11.0	1.9	2.0
Myoglobin (M-0380)	Horse skeletal muscle	18 800	7.3	1.9	2.1
Hemoglobin (H-4632)	Horse	64 650	7.0	3.2	–

[a] Sigma lot numbers given in parentheses.
[b] Stokes radius, from Ref. [9].
[c] Viscosity radius, from Ref. [10].

Table 2
Characteristics of starburst dendrimers

Generation	M_r^a	R_S^b (nm)	R_η^c (nm)
0.5	924	0.95	–
1.5	2173	1.3	–
2.5	4672	1.5	1.5
3.5	9670	2.5	1.9
4.5	19 666	3.1	2.5
5.5	39 657	3.7	3.1
6.5	79 639	4.5	4.0

[a] From supplier (MMI).
[b] From Ref. [11], in pH 7.0, 0.3 *M* phosphate buffer, via diffusion coefficient by quasi-elastic light scattering (QELS).
[c] From Ref. [12], measured in pH 5.0, 0.38 *M* phosphate buffer.

cal plate number of 40 000 m^{-1} was used throughout the study. A Rheodyne 0.2 μm filter was used to protect the column. A Milton–Roy miniPump (Riviera Beach, FL, USA) was used with a Rheodyne injector (Cotati, CA, USA) with a 100- μl injection loop. A Gilson UV detector (254 nm) in series with a Millipore–Waters differential refractometer R401 was coupled to a Kipp and Zonen two-channel recorder. The flow rate, typically 0.43 ml/min, was measured by weighing the eluent over a timed period. The buffer pH and ionic strength were confirmed with an Orion pH/millivolt meter 811 and a YSI Conductivity Bridge (Model 31), respectively.

The samples (proteins, pullulans, Ficolls, and dendrimers) were dissolved in the buffer solution by the following procedure: after preliminary mixing with a Vortex Genie (Fisher Scientific), complete dissolution was carried out with a shaker (Thermolyne Speci-mix, Sybron) or a tumbler (Labquake). Samples were filtered (0.45 mm Gelman) prior to injection. K_{SEC} was calculated using Eq. 2 with V_0 determined from pullulan P-1600 ($M_r = 1.66 \cdot 10^6$) and V_t determined from D_2O. Typical values for V_t and V_0 were 20.44 ± 0.04 ml and 7.10 ± 0.08 ml, respectively. Every run was accompanied by at least one measurement with P-1600 and D_2O on the same day.

Superose 12 pH titration

In order to protonate all carboxylate groups on the surface of the gel, about 5 g of Superose 12 column material was acid-washed thoroughly for more than 3 h by tumbling in excess 0.5 *M* HCl. The excess acid was removed by washing with water at least 30 times until the pH of the top layer became constant (pH = 5.11). The washed gel was dried in an oven over anhydrous $CaSO_4$ at 45°C for more than two days.

362.2 mg of dried gel was suspended in 10.004 g of water (HPLC grade), then degassed by N_2 for 10 min. A layer of N_2 was maintained on the liquid surface throughout the titration process. The gel was titrated using a 0.2 ml microburet

Table 3
Characteristics of ficoll fractions

Fraction	$M \times 10^{-3}$ [a]	$M_n \times 10^{-3}$ [a]	M_w/M_n	$[\eta]$ (cm^3/g)	R_S [b] (nm)	R_η [c] (nm)
T1800, Fr. 9	714	337	2.12	20.0[d]	17	13.1
T1800, Fr. 12	461	257	1.79	17.5[e]	13	10.9
T1800, Fr. 15	321	224	1.43	16.2[d]	11	9.4
T1800, Fr. 20	132	113.7	1.16	12.6[d]	7.1	6.4
T2580 IVB, Fr. 2	71.8	64.6	1.11	9.9[d]	–	4.8
T2580 IVB, Fr. 11	21.8	20.3	1.07	7.0[e]	3.0	2.9

[a] From supplier.
[b] From Ref. [11], in pH 7.0, 0.3 *M* phosphate buffer, via diffusion coefficient by quasi-elastic light scattering (QELS).
[c] From columns 2 and 5, via Eq. 5.
[d] From Ref. [13], measured at 25°C in water.
[e] By extrapolation from other data in this column using $[\eta] = 0.35 \times M_r^{0.30}$.

Table 4
Characteristics of pullulan standards

Grade	$M_r \times 10^{-3}$ [a]	M_r/M_n [a]	$[\eta]$ (cm^3/g)	R_S^b (nm)	R_η^c (nm)
P-1600	1660	1.19	306[d]	–	43.2
P-400	380	1.12	115.5	17.6	19.1
P-200	186	1.13	70.4	12.8	12.8
P-100	100	1.10	45.9	8.8	9.0
P-50	48	1.09	28.6	6.1	6.0
P-20	23.7	1.07	18.1	4.0	4.1
P-10	12.2	1.06	11.9	3.0	2.9
P-5	5.8	1.07	7.9	2.1	1.9

[a] From manufacturer (Showa Denko K.K.), in water at 25°C.
[b] From Ref. [11], in pH 7.0, 0.3 *M* phosphate buffer, via diffusion coefficient by quasi-elastic light scattering (QELS).
[c] Calculated from columns 2 and 4 via Eq. 5.
[d] By extrapolation from other data in this column using.

(Gilmont) with 0.10 *M* NaOH from the initial pH value to pH 10. The same amount (by weight) of water was used for blank titrations: an acid blank titrated with 0.103 *M* HCl (calibrated against 0.10 *M* NaOH) and a base blank with 0.10 *M* NaOH. All titrations were carried out using an Orion Research microprocessor pH/millivolt meter (Model #811) with a Beckman combination electrode (Model #39846).

Calculation of Superose 12 surface charge density (σ_s)

A calibration plot of K_{SEC} versus R is given in Fig. 2. The linearity of the plot of $K_{SEC}^{1/2}$ versus R_η supports the cylindrical pore model and allows the calculation of the pore radius (r_p) according to Eq. 3. The second linear region in the plot at large K_{SEC} is attributed to very small pores which will appear non-existent to solute molecules with $R > 2$ nm. The pore radius calculated from an average of the two slopes is 16 nm, which is in good agreement with the value of 14 nm obtained by Potschka [10]. The pore volume, V_p, was calculated using:

$$V_p = V_t - V_0 \quad (6)$$

to give a value of 13.55 ml. The actual column volume, V_c, was calculated using:

$$V_c = \pi r^2 L \quad (7)$$

where L is the length of the column (29.3 cm) and r is the inner radius of the column (0.5 cm) to give a value of 23.6 ml. The mass of Superose 12 per unit volume for a packed column is 0.23 g/ml [14]. Thus the total mass of Superose gel in the column was 23.6 ml × 0.23 g/ml = 5.4 g. The total pore area, A_p, was obtained from $V_p/A_p = r_p/2$, giving a column pore area of $2V_p/r_p = 1.7 \cdot 10^3$ m^2. The pore area per gram was thus $1.7 \cdot 10^3$ $m^2/5.4$ g = 310 m^2/g. During the titration, 362.2 mg dry gel was used, giving a total pore

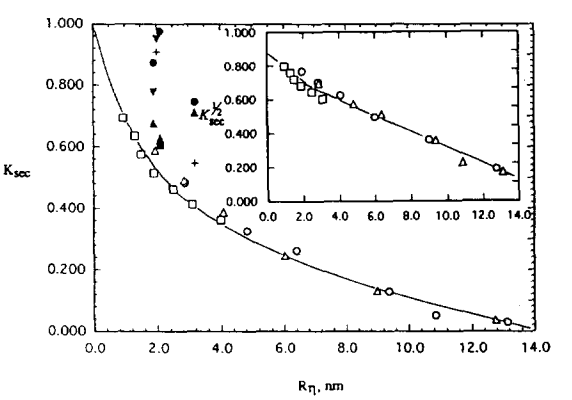

Fig. 2. Dependence of K_{SEC} on protein radius. The insert shows the ideal curve generated from data for pullulan (△), Ficoll (○), and dendrimers (□) at pH 4.0 in 400 m*M* buffer. Proteins were run at pH 5.0 in various ionic strengths: 16 m*M* (●), 66 m*M* (▲), 84 m*M* (■), 200 m*M* (▼), and 500 m*M* (+).

area involved in the titration of 0.3622 g × 310 $m^2/g = 110\ m^2$.

Finally, the column surface charge density, σ_s (C/m^2), was calculated by:

$$\sigma_s = \frac{N(V_s - V_b) \cdot N_A \cdot e}{110} \quad (8)$$

where N is the normality (molarity) of the NaOH used in the titration, V_s is the volume of NaOH consumed in the sample titration, V_b is the volume of NaOH consumed in the blank titration, N_A is Avogadro's number, and e is the electronic charge in Coulombs. The $N(V_s - V_b)$ term gives the number of equivalents of carboxyl groups on the surface of the gel.

Computer modeling

Structures for lysozyme (1hel), ribonuclease (7rsa), myoglobin (5mbn), and hemoglobin (2dhb) were imported from the Brookhaven Protein Databank to the Insight II molecular modeling system (Biosym Technologies, San Diego, CA, USA). The structures were set to pH 5.0 using the Set pH option in Biopolymer module which assigns charges to residues based on comparison with their pK_a values. A DelPhi electrostatics calculation was run and positive potential contours were displayed in order to qualitatively determine the most positive patch on the protein surface. Residues were then colored red, blue, or white according to positive, negative, or neutral formal charges, respectively, and graphic displays were printed out from the Insight II molecular modeling system.

3. Results and discussion

The curve in Fig. 2 shows the dependence of K_{SEC} on solute radius for pullulan, Ficoll, and dendrimers all in 0.4 M NaH_2PO_4–Na_2HPO_4 at pH 4.0. Data for proteins, at pH 5.0 and ionic strength ranging from 16.8 mM to 500 mM are shown by filled symbols. From Fig. 2, the K_{SEC} values for the proteins all deviated from the "ideal calibration curve". The positive deviations reveal electrostatic attraction between charged proteins and the weakly anionic Superose 12 packing surface.

A parameter analogous to k' in IEC needs to be defined in order to compare SEC data to the KRFR and the SJH models. Initially, ΔK, the vertical deviation between K_{SEC} of the solute and K_i (K_{SEC} of an "ideal" solute of the same size as the solute of interest) was used as this parameter. However, ΔK only measures the difference in the partition coefficients between proteins and "ideal" polymers and it does not isolate the free energy of interaction (ΔG_{int}) involved in the attraction between two charged surfaces. Potschka [15] has used the parameter ΔR, the horizontal displacement from the ideal curve, to describe repulsion in SEC; for attractive interactions, a negative value of ΔR may provide some measure of the magnitude of the non-ideal interaction [16] but has no physical meaning. We define K_{int}, which is analogous to k', as:

$$K_{int} = \left(\frac{C_b}{C_f}\right) \quad (9)$$

where C_b is the concentration of bound protein and C_f is the concentration of free protein in the pore. In ideal SEC, C_b is zero and K_{int} is also zero. K_{int} can be measured experimentally by (see Appendix):

$$K_{int} = \left(\frac{K_{SEC}}{K_i}\right) - 1 = \left(\frac{\Delta K}{K_i}\right) \quad (10)$$

where K_i is the K_{SEC} of an "ideal" solute of the same size as the solute of interest.

In order to determine an "optimal" pH value where the value of K_{int} changes significantly with ionic strength, a function that corresponds to the Coulombic interaction between the protein and the column packing is required. The two pH-dependent variables involved in the interaction are protein net charge, Z, and column charge density, σ_s. Protein net charge is available from published titration data (for example: lysozyme, [17]) which may be either positive (pH < pI) or negative (pH > pI). Fig. 3 shows the dependence of Superose charge density, σ_s, (determined by

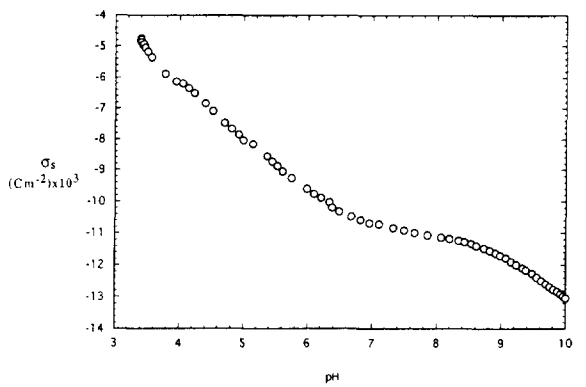

Fig. 3. Superose 12 titration curve in pure water at room temperature.

titration) on pH in pure water. (The addition of salt will shift the curve to higher σ_s but will not affect the trend shown in Fig. 4.) The product of σ_s and Z is plotted versus pH in Fig. 4 for lysozyme. The maximum of the curve in Fig. 4 should correspond to the strongest attraction between protein and packing, which in turn maximizes K_{int}.

Proteins were therefore eluted at pH 5.0 over an extended ionic strength range (16.8 mM to 500 mM) to examine the effect of ionic strength on protein retention. Table 5 lists the values of K_{int}, K_i, and Debye length (κ^{-1}) for the proteins at different ionic strength. All proteins show weaker attraction as ionic strength increases.

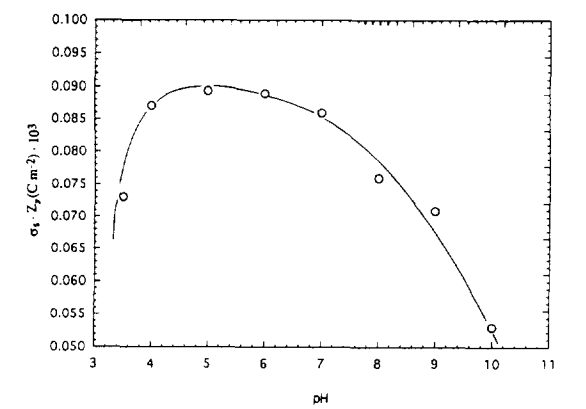

Fig. 4. Column charge density (σ_s) multiplied by lysozyme net charge (Z) versus pH.

Comparison with the KRFR model

The KRFR model predicts a linear dependence of ln k′ with ln $(1/I)$ and indicates that Z_p, the number of charged sites on a protein that interact with the packing surface, is given by the slope. Fig. 5 shows the relations between ln K_{int} and ln $(1/I)$ for four proteins, all of which appear to display two different slopes with a break point near 100 mM. Table 6 lists the two Z_p values for each protein obtained from the different slopes. Although the trend of the results is reasonable in that there is stronger electrostatic attraction at lower ionic strength, the values are excessively small. In particular, lysozyme was strongly attracted to the column (retention time ~ 2 h at $I = 27$ mM), which is difficult to reconcile with a partial charge of $+0.5$ controlling the interaction. Fig. 6 shows the most positive sides of the four proteins used in this study, with the positive residues colored black, from which it is apparent that the low values for Z_p are unreasonable. A possible interpretation is that the low charge density of Superose compared to that of the protein does not allow each protein charge to interact with a corresponding column charge.

Comparison with the SJH model

Linear dependence of ln k' on $1/\sqrt{I}$ over a moderate ionic strength range (250 m$M < I <$ 1000 mM) is predicted by the SJH model. Fig. 7 shows the dependencies of ln K_{int} on $1/\sqrt{I}$ for four proteins over an ionic strength range of 16.8 mM to 500 mM. Two proteins, lysozyme and hemoglobin, appear to be in agreement within experimental error with the prediction of the SJH model. However, for the proteins, ribonuclease and myoglobin, linearity is lost at low ionic strength.

According to the SJH model, protein charge can be calculated via the equation:

$$q_{chr} = \sqrt{\frac{SA^{\circ}_p}{135}} \tag{11}$$

where S is the slope of the ln k' versus $1/\sqrt{I}$ plot when I is in M, A°_p is the protein surface area in Å^2/molecule [18], and the constant 135 comes

Table 5
Protein K_{int} results at pH 5.0 (acetic acid buffer)

I (mM)	κ^{-1} (nm)	K_{int} [a]			
		Hemoglobin	Myoglobin	RNAse	Lysozyme
6.3	3.78	[b]	3.00	[b]	[b]
12.0	2.74	[b]	2.46	1.30	[b]
16.8	2.32	[b]	0.74	0.48	[b]
27.3	1.82	[b]	[b]	0.33	2.58
42.1	1.46	0.82	0.14	0.18	2.08
66.0	1.17	0.62	0.12	0.15	1.24
84.0	1.04	0.44	0.08	0.14	1.00
200.0	0.67	0.31	0.07	0.12	0.66
400.0	0.47	0.24	0.06	0.10	0.65
500.0	0.42	0.24	0.05	0.09	0.62

[a] $K_i = 0.44$ for hemoglobin, 0.56 for myoglobin, 0.59 for RNAse, and 0.56 for lysozyme.
[b] Values of K_{int} not reported primarily due to excessively long retention.

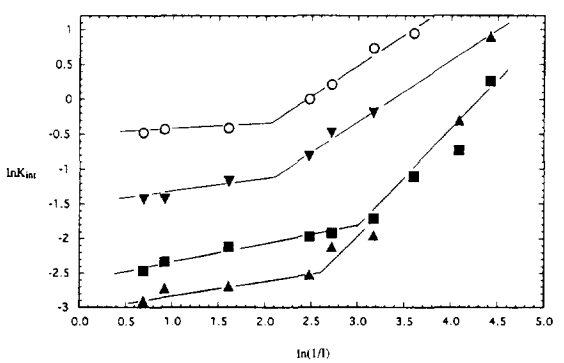

Fig. 5. Comparison with KRFR model: ln K_{int} versus ln $(1/I)$. Proteins were run at pH 5.0 in various ionic strengths as cited in Table 6: lysozyme (○), RNAse (■), myoglobin (▲), and hemoglobin (▼).

Table 6
Protein charge (Z_p) obtained according to the KRFR model, for two ranges of I

Protein	Z_p	
	5–100 mM	200–500 mM
Lysozyme	0.5	0.03
RNAse	0.7	0.14
Myoglobin	0.8	0.17
Hemoglobin	0.4	0.15

from a combination of fundamental constants. Ref. [2] indicates that this equation is only true when the column charge density is greater than the protein charge density. Our case is the opposite: protein charge density is greater than column charge density. Under these conditions, column charge density may be obtained as [2]:

$$\sigma_s = \sqrt{\frac{2\,SF(2\,RT\epsilon_0\epsilon_r)^{1/2}}{A^\circ_p}} \qquad (12)$$

where σ_s is in C/m^2 when S is the slope of the ln k' versus $1/\sqrt{I}$ plot with I in mol/m^3; F is Faraday's constant given as 96485.31 C/mol; R, the universal gas constant, is 8.314 J/mol·K; T is 298 K; ϵ_0, the permittivity of vacuum, is $8.85 \cdot 10^{-12}$ C^2/J·m; and ϵ_r is the dimensionless solvent dielectric (80). The calculated values which range from $7 \cdot 10^{-3}$ to $11 \cdot 10 - 3$ C/m^2 are in excellent agreement with the value of $8 \cdot 10^{-3}$ C/m^2 obtained at pH 5.0 from the titration curve (Fig. 3) of Superose 12.

The good agreement between our results and the SJH treatment is interesting in that SJH models the protein as a uniformly surface-charged sphere. This is diametrically opposite to the KRFR approach which emphasizes the charge heterogeneity, and specifies that k' is exclusively controlled by a few charges at one site. The SJH approach is also at variance with

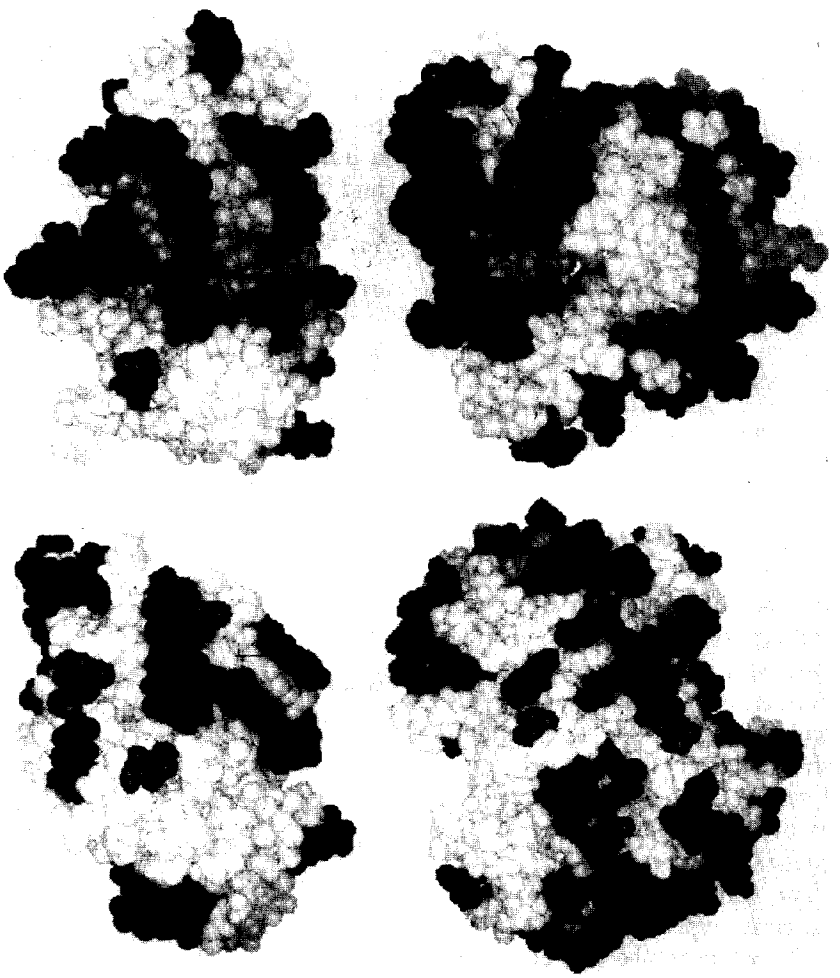

Fig. 6. Computer models of ribonuclease (upper left), myoglobin (upper right), lysozyme (lower left), and hemoglobin (lower right) at pH 5.0. Black, grey, and white indicate positive, negative, and neutral charged residues, respectively. It should be noted that these structures are not drawn to scale.

the observation that proteins are often retained on IEC columns whose charge is of the same sign as the net protein charge. It is possible that the SJH treatment works best on weak ion-exchange resins (such as that used here) to which the protein does not bind in a unique orientation; if all orientations contribute to k', then the global protein charge may be the dominant factor. On the other hand, the KRFR treatment might be somewhat more realistic in the case of strong IEC columns in low-ionic strength media, wherein one particular protein orientation corresponds to a pronounced energy minimum. In this case, a relatively small number of charged residues could control binding.

4. Conclusion

Experimental data were compared to two semi-empirical expressions for the dependence of protein retention (k') on ionic strength (I). The two corresponding theories differ in both the form of the dependence of k' on I, as well as the

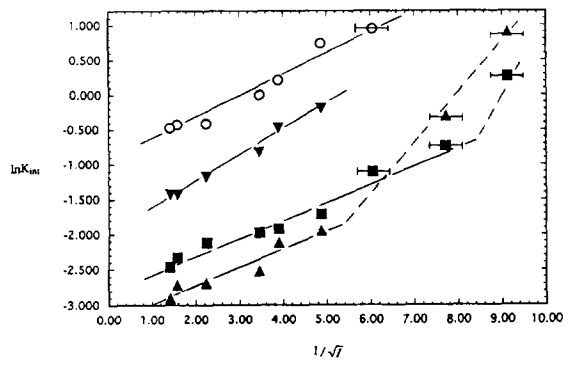

Fig. 7. Comparison with SJH model: ln K_{int} versus $(1/\sqrt{I})$. Proteins were run at pH 5.0 in various ionic strengths as cited in Table 6: lysozyme (○), RNAse (■), myoglobin (▲), and hemoglobin (▼).

method for calculation of the protein and/or packing charge. The KRFR model does not conform to our results with respect to either the form of the dependence or the calculation of the protein charge. The SJH model agrees with the shape of the dependence of k' on I, and yields therefrom a calculated value for the column packing surface charge density in agreement with the experimental result.

The predictions offered in the context of the SJH theory are presented for two cases: $\sigma_s > \sigma_p$ and $\sigma_s < \sigma_p$ [2]. The validity of the theory was earlier checked against experimental data only for the first case [2], while in the present work the latter case alone was studied. Further experimental work should be carried out over a wider range of σ_s and σ_p, especially at values of σ_s near σ_p, in order to provide a more complete test of the SJH model.

Acknowledgment

This work was supported by NSF grant No. CHE-9021484. We thank Dr. K. Granath for the Ficoll fractions and Dr. Lars Hagel for the Superose column. We also thank Daniel Robertson of the Facility for Computational Molecular and Biomolecular Science at Indiana University–Purdue University for his assistance with the computer modeling.

Appendix

The desired quantity is related to the interaction energy, ΔG_{int}, for the binding (adsorption) of a protein to the column packing. Within a pore of the packing, the concentration of free and bound protein are related by:

$$C_b = C_f e^{-\Delta G_{int}/RT} \tag{A1}$$

or

$$K_{int} = \left(\frac{C_b}{C_f}\right). \tag{A2}$$

In ideal SEC, C_b is zero, therefore K_{int} is zero. In non-ideal SEC, the total concentration of protein in the pore is given by:

$$C_p = C_b + C_f. \tag{A3}$$

The observed elution volume is given by:

$$V_{obs} = V_0 + K_{SEC}\, V_p \tag{A4}$$

where K_{SEC} is the relative probability of the protein being inside the pore, given by:

$$K_{SEC} = \frac{C_p}{C_0} \tag{A5}$$

where C_0 is the concentration of the protein in the mobile phase. For ideal SEC,

$$V_i = V_0 + K_i V_p \tag{A6}$$

where K_i is given by:

$$K_i = \frac{C_p}{C_0}. \tag{A7}$$

Under non-ideal conditions, $K_i = C_f/C_0$. From Eq. A2,

$$K_{int} = \frac{C_b}{C_f} = \frac{C_b/C_0}{C_f/C_0} = \frac{C_p/C_0}{C_f/C_0}(C_b/C_p) = \frac{K_{SEC}}{K_i} \cdot \frac{C_b}{C_p} \tag{A8}$$

and from Eq. A3,

$$\frac{C_b}{C_p} = \frac{C_b}{C_b + C_f} = \frac{C_b/C_f}{(C_b/C_f) + 1} = \frac{K_{int}}{K_{int} + 1} \tag{A9}$$

Now, by substituting A9 into A8, we get:

$$K_{int} = \frac{K_{SEC}}{K_i}\left(\frac{K_{int}}{K_{int}+1}\right) \quad \text{(A10)}$$

This by rearrangement gives:

$$K_{int} = \frac{K_{SEC}}{K_i} - 1 = \frac{\Delta K}{K_i} \quad \text{(A11)}$$

References

[1] W. Kopaciewicz, M.A. Rounds, J. Fausnaugh and F.E. Regnier, *J. Chromatogr.*, 283 (1984) 37.

[2] J. Ståhlberg, B. Jönsson and Cs. Horváth, *Anal. Chem.*, 63 (1991) 1867.

[3] See, for example, K. Gooding and F. Regnier (Editors), *High Performance Liquid Chromatography of Biological Macromolecules: Methods and Applications*, Marcel Dekker, New York, 1988.

[4] N.K. Boardman and S.M. Partridge, *Biochem. J.*, 59 (1955) 543.

[5] V. Lesins and E. Ruckenstein, *J. Colloid Interface Sci.*, 132 (1989) 566.

[6] W. Kopaciewicz and F.E. Regnier, *Nonideal Size-Exclusion Chromatography of Proteins: Effects of pH at Low Ionic Strength*, paper presented at the *International Symposium on HPLC of Proteins and Peptides, November 16–17, 1981, Washington D.C.*

[7] H. Waldmann-Mayer, *J. Chromatogr.*, 350 (1991) 1.

[8] P.J. Flory, *Principles of Polymer Chemistry*, Cornell University Press, Ithaca, NY, 1953, p. 606.

[9] M. le Maire, A. Ghazi, J.V. Moller and L.P. Aggerberk, *Biochem. J.*, 243 (1987) 399.

[10] M. Potschka, *J. Chromatogr.*, 587 (1991) 276.

[11] P.L. Dubin, S.L. Edwards, M.S. Mehta, and D. Tomalia, *J. Chromatogr.*, 635 (1993) 51.

[12] P.L. Dubin, S.L. Edwards, M.S. Mehta, J.I. Kaplan and J. Xia, *Anal. Chem.*, 64 (1992) 2344.

[13] G. Shah and P. Dubin, unpublished results.

[14] K. Fjarstedt, Pharmacia Biotech, private communication.

[15] M. Potschka, *J. Chromatogr.*, 441 (1988) 239.

[16] S.L. Edwards and P.L. Dubin, *J. Chromatogr.*, 648 (1993) 3.

[17] C. Tanford, *J. Am. Chem. Soc.*, 76 (1956) 3331.

[18] J. Ståhlberg, Astra Pharmaceutical, private communication.